The EMBO Journal vol.14 no.7 pp.1520–1531, 1995

Cloning and characterization of hTAF$_{II}$18, hTAF$_{II}$20 and hTAF$_{II}$28: three subunits of the human transcription factor TFIID

Gabrielle Mengus, Michael May, Xavier Jacq, Adrien Staub, Laszlo Tora, Pierre Chambon and Irwin Davidson[1]

Institut de Génétique et de Biologie Moléculaire et Cellulaire, CNRS/INSERM/ULP, Collège de France, BP 163-67404 Illkirch Cédex, France

[1]Corresponding author

Communicated by P.Chambon

We have cloned cDNAs encoding three novel TAF$_{II}$s [TATA-binding protein (TBP)-associated factors] from the human (h) HeLa cell TFIID complexes hTAF$_{II}$28, hTAF$_{II}$20 and hTAF$_{II}$18. hTAF$_{II}$28 is a core hTAF$_{II}$ present in both of the previously described hTFIID species which either lack or contain hTAF$_{II}$30 (hTFIIDα and hTFIIDβ respectively), and is the homologue of *Drosophila* (d)TAF$_{II}$30β. hTAF$_{II}$18 is a novel hTAF$_{II}$ which shows homology to the N-terminal region of the yeast TAF$_{II}$ SPT3, but has no known *Drosophila* counterpart. In contrast to hTAF$_{II}$28, hTAF$_{II}$18 is a TFIIDβ-specific hTAF$_{II}$. hTAF$_{II}$20 is the homologue of p22, an alternatively spliced form of dTAF$_{II}$30α (p32). Using a combination of protein affinity chromatography and cotransfection and immunoprecipitation assays, we have identified a series of *in vitro* and intracellular interactions among the novel hTAF$_{II}$s and between the novel hTAF$_{II}$s and hTAF$_{II}$30 or TBP. We show that hTAF$_{II}$28 interacts with hTAF$_{II}$18 both *in vitro* and intracellularly; in contrast to its *Drosophila* homologue, hTAF$_{II}$28 also interacts directly with TBP. Deletion analysis indicates that TBP and hTAF$_{II}$18 bind to distinct domains of hTAF$_{II}$28. hTAF$_{II}$18 also interacts with TBP, but it interacts more strongly with hTAF$_{II}$28 and hTAF$_{II}$30. The binding of hTAF$_{II}$28 and hTAF$_{II}$30 requires distinct domains of hTAF$_{II}$18. As observed with the homologous *Drosophila* proteins, hTAF$_{II}$20 interacts directly with TBP; however, additional interactions between hTAF$_{II}$20 and hTAF$_{II}$28 or hTAF$_{II}$30 were detected. These results reveal differences not only in subunit composition, but also in the organization of dTFIID and hTFIID complexes.

Key words: *Drosophila* TAF$_{II}$s/protein–protein interactions/RNA polymerase II transcription factors/TBP-associated factors (TAF$_{II}$)/yeast TAF$_{II}$s

Introduction

Regulated transcription by RNA polymerase II requires the formation of multiprotein preinitiation complexes at the promoters of transcribed genes. These multiprotein complexes comprise RNA polymerase II, factors required for basal transcription from minimal promoters *in vitro* [TFIIB, TFIIE, TFIIF, TFIIH and the TATA-binding protein (TBP)] (for reviews see Roeder, 1991; Conaway and Conaway, 1993; Buratowski, 1994, and references therein), and factors required for regulated transcription, such as TFIIA and TFIID (DeJong and Roeder, 1993; Ma *et al.*, 1993; Yokomori *et al.*, 1993a, 1994; Lieberman and Berk, 1994; Ozer *et al.*, 1994; Sun *et al.*, 1994; and see above reviews). The activity of the basal transcription machinery can be modulated by transactivator proteins bound to *cis*-acting regulatory elements located upstream or downstream of the transcription start site. Some transactivators interact directly *in vitro* with components of the basal preinitiation complex (e.g. TBP, TFIIB and TFIIH; see Hernandez, 1993; Tjian and Maniatis, 1994, and references therein). However, transcriptional activation also appears to require coactivators, for example the yeast ADA proteins and the mammalian CBP or PC4 proteins, which may act as bridging molecules linking transactivators to the basal transcription factors (Arlas *et al.*, 1994; Ge and Roeder, 1994; Kretzschmar *et al.*, 1994a,b; Kwok *et al.*, 1994; Marcus *et al.*, 1994). Such coactivators can be separated easily from the basal transcription factors, while others are tightly associated with TBP in the TFIID complex [TBP-associated factors (TAF$_{II}$s); reviewed in Gill and Tjian, 1992; Pugh and Tjian, 1992; Hernandez, 1993; Tjian and Maniatis, 1994].

The TAF$_{II}$ composition of TFIID complexes from *Drosophila* embryos (dTAF$_{II}$s) and human HeLa cells (hTAF$_{II}$s) has been determined (Dynlacht *et al.*, 1991; Pugh and Tjian, 1991; Tanese *et al.*, 1991; Timmers *et al.*, 1992; Zhou *et al.*, 1992, 1993; Brou *et al.*, 1993a; Chiang *et al.*, 1993; Kokubo *et al.*, 1993a), and cDNAs encoding many of the dTAF$_{II}$s have been cloned (Dynlacht *et al.*, 1993; Goodrich *et al.*, 1993; Hisatake *et al.*, 1993; Hoey *et al.*, 1993; Kokubo *et al.*, 1993b, 1994; Ruppert *et al.*, 1993; Weinzierl *et al.*, 1993a,b; Yokomori *et al.*, 1993b; Verrijzer *et al.*, 1994). Recombinant dTAF$_{II}$250 (Ruppert *et al.*, 1993; designated p230 in Hisatake *et al.*, 1993) and dTAF$_{II}$30α (Yokomori *et al.*, 1993b; p28 in Kokubo *et al.*, 1994) interact directly with dTBP, whereas others are recruited to TFIID by TAF–TAF interactions (Weinzierl *et al.*, 1993a,b; Chen *et al.*, 1994). Functional analysis has revealed that some TAF$_{II}$s may function as bridging molecules required for the activity of transcriptional activators. dTAF$_{II}$110 (p110 in Kokubo *et al.*, 1993b) interacts directly with the transcriptional activator Sp1 *in vitro* (Hoey *et al.*, 1993; Gill *et al.*, 1994). On the other hand dTAF$_{II}$40 (p42 in Kokubo *et al.*, 1994) interacts with the acidic activator VP16 and with the basal transcription factors TBP and TFIIB, thus forming a ternary complex between a transactivator and two components of the basal transcription complex (Goodrich *et al.*, 1993). In hTFIID, a direct interaction between hTAF$_{II}$30 and the region of the oestrogen receptor (ER), which harbours the activation

function 2a active in yeast (AF-2a; Pierrat *et al.*, 1994), has been detected *in vitro* (Jacq *et al.*, 1994). Furthermore, the hTFIID species containing $hTAF_{II}30$ was shown to be required for a ligand-independent ER AF-2 activity *in vitro* (Jacq *et al.*, 1994). These results support the idea that transcriptional activation involves direct contacts between transcriptional activators and TAF_{II}s, and that different TAF_{II}s may mediate the function of distinct transcriptional activators (Chen *et al.*, 1994).

At present cDNAs encoding the human homologues of two dTFIID subunits, $hTAF_{II}250$ ($dTAF_{II}250$, identical to the product of the CCG1 gene; Sekiguchi *et al.*, 1991; Hisatake *et al.*, 1993; Ruppert *et al.*, 1993) and $hTAF_{II}70$ ($dTAF_{II}60$; Weinzierl *et al.*, 1993b), have been cloned. The amino acid sequences of these *Drosophila* and human TAF_{II}s are highly conserved, and analogous TAF–TAF and TAF–TBP interactions have been observed in *Drosophila* and human TFIID with these TAF_{II}s. However, despite these similarities, differences between human and *Drosophila* TFIID have been noted. hTFIID appears to comprise more subunits than dTFIID (Brou *et al.*, 1993a; Chiang *et al.*, 1993). This was confirmed by the isolation of the cDNA encoding $hTAF_{II}30$, for which no *Drosophila* homologue is known (Jacq *et al.*, 1994). Moreover, all of the $dTAF_{II}$s isolated from *Drosophila* embryos appear to be present in a single TFIID species, whereas we have shown previously that HeLa cells contain several chromatographically separable TFIID complexes with distinct functional properties (Brou *et al.*, 1993a,b). Further, we have shown that the TFIID complexes present in HeLa cell nuclear extracts can be separated into two species, which either lack (designated hereafter hTFIIDα) or contain (hTFIIDβ) $hTAF_{II}30$ (Jacq *et al.*, 1994). Interestingly, hTFIIDα and hTFIIDβ were found to differ further in their subunit composition. $hTAF_{II}17$ (designated hereafter $hTAF_{II}18$), 20, 37 and 125 appeared to be preferentially associated with hTFIIDβ, and $hTAF_{II}29$, 64, 106 and 150 appeared to be preferentially associated with hTFIIDα. In contrast, $hTAF_{II}28$, 60, 85, 100, 135 and 250 were detected in both TFIIDα and TFIIDβ (Jacq *et al.*, 1994; Figure 3A). It appears, therefore, that $hTAF_{II}$s can be divided into (i) common (core) TAF_{II}s present in both the TFIIDα and TFIIDβ complexes, and (ii) specific $hTAF_{II}$s which are selectively present in hTFIIDα or hTFIIDβ.

We report here the isolation of cDNAs encoding three novel subunits of HeLa cell TFIID: $hTAF_{II}28$, $hTAF_{II}20$ and $hTAF_{II}18$. $hTAF_{II}28$ is a core TAF_{II} present in both hTFIIDα and hTFIIDβ, and is the homologue of $dTAF_{II}30\beta$, while $hTAF_{II}20$ is the homologue of p22 (Kokubo *et al.*, 1994), an alternatively spliced form of $dTAF_{II}30\alpha$. In contrast, $hTAF_{II}18$ is a novel TAF_{II} with no known *Drosophila* counterpart, and is preferentially associated with hTFIIDβ. Using a combination of *in vitro* and intracellular protein–protein interaction assays, we have determined multiple specific TAF–TAF and TAF–TBP interactions amongst the newly cloned $hTAF_{II}$s and between the novel $hTAF_{II}$s and $hTAF_{II}30$.

Results

cDNAs encoding $hTAF_{II}18$, $hTAF_{II}20$ and $hTAF_{II}28$

TFIID complexes were partially purified from HeLa cell nuclear extracts by chromatography on a heparin–ultrogel column (Brou *et al.*, 1993a; Chaudhary *et al.*, 1994), and the TFIID was immunopurified from the 0.6 M KCl fraction using an anti-TBP mAb (Jacq *et al.*, 1994; see Materials and methods). Following SDS–PAGE, the $hTAF_{II}$s were transferred to a polyvinylidine difluoride (PVDF) membrane and the 28, 20 and 18 kDa subunits (see Figure 3A), corresponding to putative core and specific $hTAF_{II}$s (see Introduction), were digested with trypsin. The resulting peptides were separated by reverse-phase chromatography, and several peptide sequences were obtained for each protein (listed in Materials and methods).

Degenerate oligonucleotides based on these peptide sequences were used to screen a random-primed HeLa cell cDNA library. Three clones hybridizing to the two oligonucleotide probes derived from $hTAF_{II}28$ were isolated and their DNA sequences determined (Figure 1A). The deduced open reading frame (ORF) encodes a 211 amino acid protein, with a calculated molecular mass of 27.1 kDa containing both of the tryptic peptides derived from the purified HeLa cell $hTAF_{II}28$ subunit (underlined in Figure 1A). Comparison with the previously identified $dTAF_{II}$s indicated that $hTAF_{II}28$ is the homologue of $dTAF_{II}30\beta$ (Yokomori *et al.*, 1993b; Figure 1B). The human and *Drosophila* proteins are 50% identical overall, with the C-terminal region being better conserved than the N-terminal region (Figure 1B).

Two oligonucleotide probes derived from $hTAF_{II}20$ peptides were used to screen the HeLa cell cDNA library, and six clones were isolated. The cDNA sequence (Figure 1C) contains an ORF of 161 amino acids encoding a protein with a calculated molecular mass of 20.7 kDa, comprising the four tryptic peptide sequences obtained from the purified $hTAF_{II}20$ subunit (Figure 1C). Comparison with the $dTAF_{II}$s indicated that $hTAF_{II}20$ is the homologue of p22 (Kokubo *et al.*, 1994), an alternatively spliced form of $dTAF_{II}30\alpha$ (Yokomori *et al.*, 1993b). The human and *Drosophila* proteins are 53% identical and, as observed for $hTAF_{II}28$ and $dTAF_{II}30\beta$, the homology is higher in the C-terminal region than in the N-terminal region (Figure 1D).

Five clones hybridizing to oligonucleotides derived from the purified $hTAF_{II}18$ subunit were isolated and sequenced. The cDNA encodes a 124 amino acid protein of 16.5 kDa comprising both of the tryptic peptide sequences derived from the endogenous $hTAF_{II}18$ (Figure 2A). Comparison of the sequence of $hTAF_{II}18$ with those of the $dTAF_{II}$s did not reveal any similarity. Thus, $hTAF_{II}18$ appears to be a novel human TAF_{II}. However, a fastaA (Pearson and Lipman, 1988) search of the Swiss Prot database revealed that the amino acid sequence of $hTAF_{II}18$ shares homology with two yeast proteins. $hTAF_{II}18$ is 28% identical (59% similarity) to the yeast protein FUN 81 (Dubois *et al.*, 1987; Figure 2B). This protein has been shown to be essential for vegetative yeast growth, but its function is unknown. FUN 81 may therefore be a yeast TAF_{II}. Interestingly, $hTAF_{II}18$ is also 26.5% identical (48% similarity) to the N-terminal region (amino acids 2–102) of the yeast TAF_{II} SPT3 (Eisenmann *et al.*, 1992; Figure 2C).

$hTAF_{II}18$ is preferentially associated with TFIIDβ, whereas $hTAF_{II}28$ is a core TAF_{II}

To determine the distribution of the novel $hTAF_{II}$s in the TFIIDα and TFIIDβ species (i.e. lacking or containing

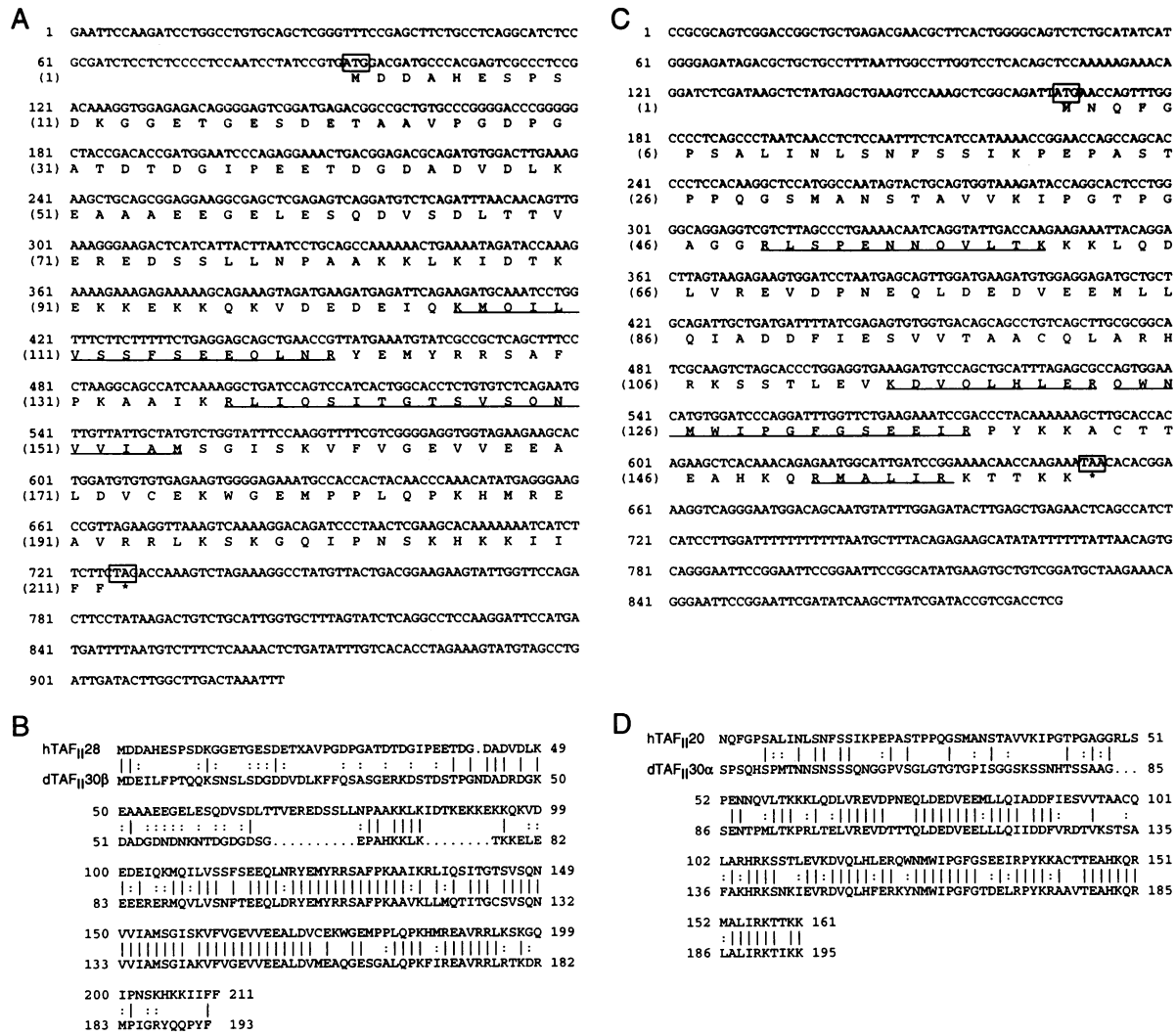

Fig. 1. (**A**) Nucleotide and amino acid sequences of hTAF$_{II}$28. The numbers to the left indicate the nucleotides and those in brackets the amino acids. The two tryptic peptides derived from the endogenous HeLa cell TAF$_{II}$28 are underlined. (**B**) Comparison of the amino acid sequences of hTAF$_{II}$28 and dTAF$_{II}$30β. The amino acid sequences of the two proteins were compared using the 'bestfit' programme of the Genetics Computer Group (GCG, University of Wisconsin, WI) software package. The upper line shows the sequence of hTAF$_{II}$28 and the lower that of dTAF$_{II}$30β. The bars indicate identical amino acids, and the dots similar amino acids. (**C**) Nucleotide and amino acid sequences of hTAF$_{II}$20. The organization is as in (A). The tryptic peptides from the endogenous HeLa cell TAF$_{II}$20 are underlined. (**D**) Comparison of the amino acid sequences of hTAF$_{II}$20 and dTAF$_{II}$30α. The hTAF$_{II}$20 is indicated on the upper line and dTAF$_{II}$30α on the lower line. Comparison was performed as in (B).

hTAF$_{II}$30, respectively), total TFIID was immunopurified from HeLa cell nuclear extracts using the anti-TBP mAb 3G3 (Brou *et al.*, 1993a; Lescure *et al.*, 1994; Figure 3B, TFIID, lanes 1 and 4). To separate TFIIDα from TFIIDβ, immunopurified total TFIID was reimmunoprecipitated with the anti-hTAF$_{II}$30 mAb 2F4 (Jacq *et al.*, 1994). The resulting TFIIDα and TFIIDβ were sequentially probed with mAbs against hTAF$_{II}$30 and TBP, as well as with mouse antisera raised against purified glutathione *S*-transferase (GST)−hTAF$_{II}$18 and GST−hTAF$_{II}$28 (see Materials and methods). Both hTAF$_{II}$18 and hTAF$_{II}$28 were detected along with hTAF$_{II}$30 and TBP in the total immunopurified TFIID (Figure 3B, lanes 1 and 4). As described previously (Jacq *et al.*, 1994), TBP could be detected in both TFIIDα and TFIIDβ, whereas hTAF$_{II}$30 was almost exclusively present in TFIIDβ (Figure 3B, lanes 2, 3, 5 and 6). Similar to TBP, hTAF$_{II}$250 and hTAF$_{II}$100 (data not shown; Jacq *et al.*, 1994), hTAF$_{II}$28 was detected in both TFIIDα and TFIIDβ (Figure 3B, lanes 4–6). In contrast, the hTAF$_{II}$18 detected in total TFIID was clearly present in TFIIDβ, but only trace amounts were detected in TFIIDα (Figure 3B, compare lanes 1–3). As we have not yet raised antibodies against hTAF$_{II}$20, its distribution in TFIIDα and β cannot be determined. These results indicate that the isolated cDNAs for hTAF$_{II}$28 and hTAF$_{II}$18 encode bona fide TAF$_{II}$s, which can be immunoprecipitated by antibodies against TBP and hTAF$_{II}$30. Moreover, as suggested previously (Jacq *et al.*, 1994), hTAF$_{II}$28 is a core TAF$_{II}$ present in both TFIIDα and TFIIDβ, whereas hTAF$_{II}$18 is a specific TAF$_{II}$ preferentially associated with TFIIDβ.

TAF–TAF and TAF–TBP interactions in vitro

We investigated whether these novel hTAF$_{II}$s interact with each other and also whether they interact with TBP, hTAF$_{II}$30 or hTAF$_{II}$250. The cDNAs encoding hTAF$_{II}$18, 20 and 28 were cloned into the pXJ series vectors (Xiao *et al.*, 1991) and translated *in vitro* (Figure 4A).

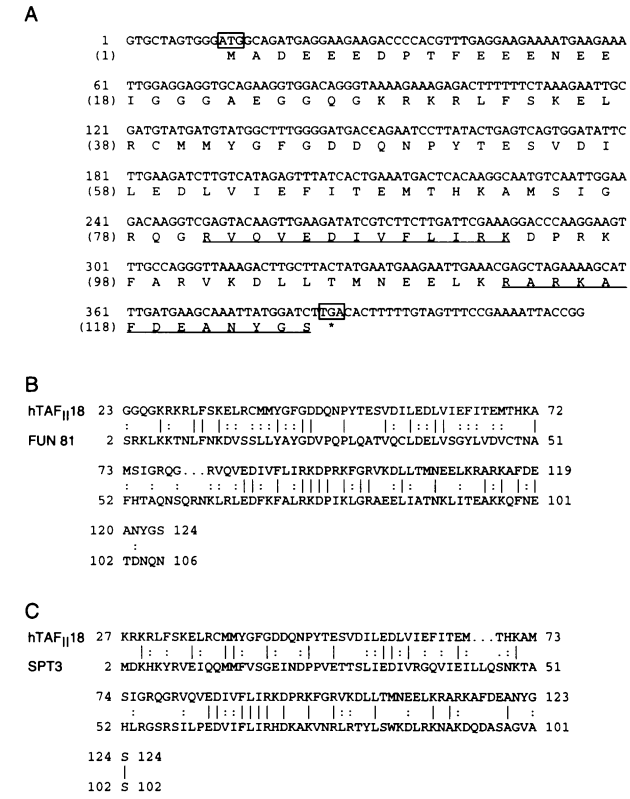

Fig. 2. (**A**) Nucleotide and amino acid sequences of hTAF$_{II}$18. Presentation is as in Figure 1A. The tryptic peptides derived from the endogenous HeLa cell TAF$_{II}$18 are underlined. (**B**) Comparison of the amino acid sequences of hTAF$_{II}$18 and FUN 81. Amino acid comparisons were performed using the 'bestfit' program as described in the legend to Figure 1B. The upper line shows hTAF$_{II}$18 and the lower line FUN 81. (**C**) Comparison of the amino acid sequences of hTAF$_{II}$18 and the yeast TAF$_{II}$ SPT3. Comparisons were performed as described in the legend to Figure 1B. The upper line shows the sequence of hTAF$_{II}$18 and the lower line the N-terminal region of SPT3.

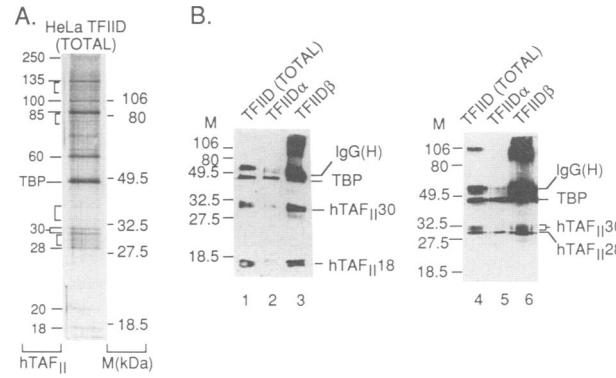

Fig. 3. (**A**) TAF$_{II}$ composition of total HeLa cell TFIID. HeLa cell TFIID was immunopurified from the heparin 0.6 M KCl fraction using the anti-TBP mAb 3G3 and elution with a synthetic peptide containing the 3G3 epitope. The immunopurified hTAF$_{II}$s were separated by SDS−PAGE and the gel stained with silver nitrate. The locations of identified hTAF$_{II}$s are indicated according to their apparent relative molecular masses in kDa. The brackets indicate other proteins which are immunopurified by mAb 3G3, but whose identity has not as yet been determined. M shows the positions of the prestained molecular mass markers. (**B**) hTAF$_{II}$28 is a core hTAF$_{II}$, whereas hTAF$_{II}$18 is a TFIIDβ-specific TAF$_{II}$. Total TFIID was purified from HeLa cell nuclear extract with mAb 3G3 (TFIID, lanes 1 and 4) and reimmunoprecipitated with 1 μg of the anti-hTAF$_{II}$30 mAb 2F4 and 30 μl of protein G−Sepharose. The immunoprecipitation supernatant contains TFIIDα (lanes 2 and 5). The immunoprecipitated TFIIDβ (lanes 3 and 6) was washed four times with buffer A containing 1.0 M KCl and separated by 12.5% SDS−PAGE (lanes 1–3) or 10% SDS−PAGE (lanes 4–6). The proteins were electrotransferred to nitrocellulose and detected first with mAbs 2C1 and 4G2 against TBP and hTAF$_{II}$30 respectively, and subsequently with the anti-hTAF$_{II}$18 serum (lanes 1–3) or the anti-hTAF$_{II}$28 serum (lanes 4–6). The positions of the molecular mass markers are indicated, along with the positions of TBP, hTAF$_{II}$30, hTAF$_{II}$28 and hTAF$_{II}$18. IgG(H) shows the position of the heavy chains of the mAbs used in the immunoprecipitations.

GST−hTAF$_{II}$28, GST−hTAF$_{II}$18 and GST−TBP were expressed in *Escherichia coli* and immobilized on glutathione−Sepharose beads (see Materials and methods). Equivalent amounts of immobilized fusion proteins were incubated with ^{35}S-labelled hTAF$_{II}$s or TBP. Following extensive washing with buffer containing either 0.1 or 0.5 M KCl (see Materials and methods), the bound proteins were subjected to SDS−PAGE and detected by autoradiography.

In vitro-translated hTAF$_{II}$28 bound strongly to GST−hTAF$_{II}$18 after washing with both 0.1 and 0.5 M KCl (Figure 4D, lanes 5 and 6 respectively), and in the reciprocal experiment hTAF$_{II}$18 bound to GST−hTAF$_{II}$28 (Figure 4C, lanes 3 and 4). As expected from previous results (Jupp *et al.*, 1993; Kato *et al.*, 1994), *in vitro*-translated TBP bound to the GST−TBP beads (Figure 4B, lanes 1 and 2). TBP also interacted with the GST−hTAF$_{II}$28 beads (Figure 4C, lanes 1 and 2), but in the reciprocal experiment only weak binding of hTAF$_{II}$28 to the GST−TBP beads was observed (Figure 4B, lanes 7 and 8). As described previously for p22 and dTAF$_{II}$30α, hTAF$_{II}$20 interacted strongly *in vitro* with GST−TBP (Figure 4B, lanes 5 and 6), but no significant interactions between hTAF$_{II}$20 and GST−hTAF$_{II}$28 or GST−hTAF$_{II}$18 could be detected (Figure 4C, lanes 5 and 6, and D, lanes 3 and 4, respectively). Furthermore, in contrast to the strong binding of hTAF$_{II}$18 to GST−hTAF$_{II}$28, only weak binding of hTAF$_{II}$18 to GST−TBP was observed (Figure 4C and B, respectively, lanes 3 and 4).

We also investigated possible interactions between the novel hTAF$_{II}$s and the hTAF$_{II}$30 and hTAF$_{II}$250 described previously. Histidine (his)-tagged hTAF$_{II}$30 was expressed in *E.coli*, purified (Jacq *et al.*, 1994) and incubated with GST−hTAF$_{II}$28, GST−hTAF$_{II}$20 and GST−hTAF$_{II}$18. No interaction between GST−hTAF$_{II}$28 and his-hTAF$_{II}$30 could be detected (Figure 4F, lanes 8 and 10), whereas his-hTAF$_{II}$30 bound to GST−hTAF$_{II}$18 (Figure 7F, lanes 1–3). His-hTAF$_{II}$30 also interacted with wild-type GST−hTAF$_{II}$20 (WT), but not with GST−hTAF$_{II}$20(1–71) in which the C-terminus of hTAF$_{II}$20 was deleted (Figure 7F, lanes 7 and 8). Furthermore, baculovirus-expressed hTAF$_{II}$250 bound to GST−TBP (and as expected also to GST−hTAF$_{II}$135, the human homologue of dTAF$_{II}$110; see Discussion), but no interactions with GST−hTAF$_{II}$28 and GST−hTAF$_{II}$18 were observed (Figure 4E, lanes 1–5).

The above results indicated that TBP bound efficiently to GST−hTAF$_{II}$28, but surprisingly little binding was seen in the reciprocal experiment. As an alternative to *in vitro* translation products, his-tagged hTAF$_{II}$28 and hTAF$_{II}$18 were expressed and purified from *E.coli*. Following

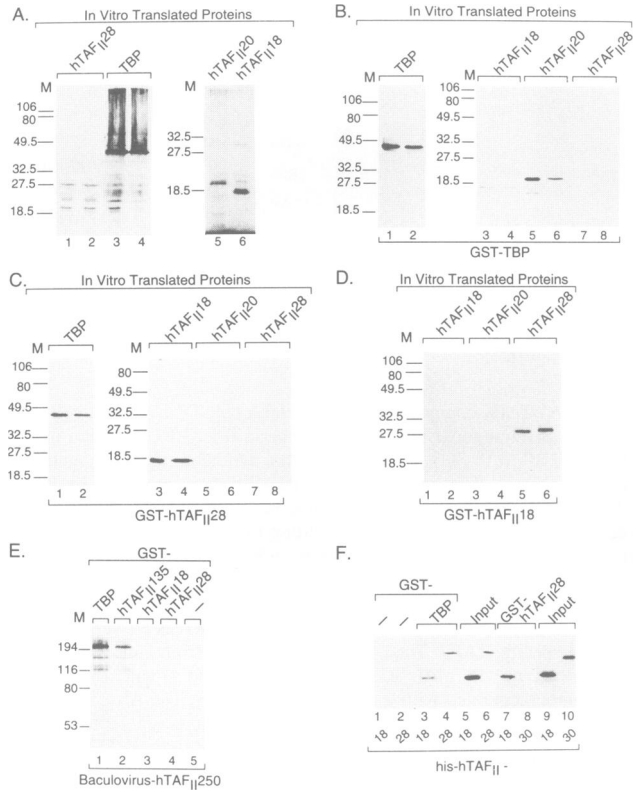

Fig. 4. (**A**) *In vitro* translation of hTAF$_{II}$s and TBP. The hTAF$_{II}$s and TBP cloned in the pXJ series vectors were transcribed *in vitro* with T7 polymerase and translated with rabbit reticulocyte lysate in the presence of [^{35}S]methionine. A 1 µl aliquot of the reaction was separated by SDS–PAGE and detected by autoradiography. In lanes 1–4 each pair of lanes shows a duplicate reaction. M indicates the positions of the molecular mass markers. (**B**) Protein affinity chromatography with GST–TBP. Approximately 2 µg of GST–TBP were immobilized on 50 µl of glutathione–Sepharose, incubated with 2 µl of *in vitro*-translated TBP and hTAF$_{II}$18, 3 µl of hTAF$_{II}$20 and 6 µl of hTAF$_{II}$28, and washed as described in Materials and methods. The bound TBP and hTAF$_{II}$s were separated on gels containing 10 or 12% acrylamide, respectively. Odd-numbered lanes show the proteins retained on the beads after the wash with 0.1 M KCl; the even-numbered lanes show the proteins retained after the 0.5 M KCl wash. (**C** and **D**) TAF–TAF and TAF–TBP interactions *in vitro*. Protein affinity chromatography was performed as described in (B) using immobilized GST–hTAF$_{II}$28 or GST–hTAF$_{II}$18. (**E**) Baculovirus hTAF$_{II}$250 binds to TBP and hTAF$_{II}$135, but not to hTAF$_{II}$28 or hTAF$_{II}$18. Protein affinity chromatography was performed using extracts from Sf9 cells infected with baculovirus expressing hTAF$_{II}$250 in the presence of [^{35}S]methionine (a generous gift from J.Acker). The extract was first adsorbed on glutathione–Sepharose to remove non-specific binding proteins. The flowthrough fraction was then incubated with the immobilized GST fusions. The resins were washed with buffer containing 0.5 M KCl and the bound proteins detected by autoradiography. (**F**) Protein affinity chromatography with purified his-hTAF$_{II}$s. Purified his-hTAF$_{II}$30, his-hTAF$_{II}$28 and his-hTAF$_{II}$18 were incubated with an ~20-fold excess of GST–TBP or GST–hTAF$_{II}$28, washed with buffer containing 0.5 M KCl, and the bound proteins detected by immunoblotting using mAbs 4G2, 15TA and 16TA, to detect hTAF$_{II}$30, 28 and 18, respectively. Lanes 1–6 and 7–10 were taken from different blots to avoid the detection of GST–hTAF$_{II}$28 in lanes 7–8 with the 15TA antibody.

quantitation by SDS–PAGE and Coomassie blue staining, equal amounts of the purified proteins were incubated with a 20- to 30-fold excess of GST–TBP. Almost all of the his-hTAF$_{II}$28 was retained on the GST–TBP beads, while only a fraction of the his-hTAF$_{II}$18 was retained (Figure 4F, lanes 3–6). However, his-hTAF$_{II}$18 bound strongly to GST–hTAF$_{II}$28, whereas no significant binding of his-hTAF$_{II}$30 was observed (Figure 4F, lanes 7–10). These results confirm that hTAF$_{II}$28 binds efficiently and directly to TBP and that hTAF$_{II}$18 interacts more efficiently with hTAF$_{II}$28 than with TBP. Moreover, in agreement with the results using the *in vitro*-translated hTAF$_{II}$20, no binding of his-hTAF$_{II}$18 or his-hTAF$_{II}$28 to GST–hTAF$_{II}$20 was observed (data not shown).

Taken together, these *in vitro* results indicate that hTAF$_{II}$28, hTAF$_{II}$20 and hTAF$_{II}$18 interact with TBP with varying affinities. In addition, hTAF$_{II}$28 interacts with hTAF$_{II}$18 but not with hTAF$_{II}$30, while both hTAF$_{II}$18 and hTAF$_{II}$20 interact with hTAF$_{II}$30. No interactions between hTAF$_{II}$250 and hTAF$_{II}$28 or hTAF$_{II}$18 could be detected.

hTAF$_{II}$28 interacts intracellularly with TBP and hTAF$_{II}$18 but not with hTAF$_{II}$30

Transient cotransfection in COS cells was used to determine whether the above *in vitro* interactions could be observed intracellularly. hTAF$_{II}$28, N-terminally tagged with the oestrogen receptor epitope B10 (B10-hTAF$_{II}$28), and recombinant TBP were revealed on Western blots of the transfected cell extracts with a mixture of mAb B10 (Ali *et al.*, 1993) and the anti-TBP mAb 3G3. B10-hTAF$_{II}$28 could be detected in extracts from cells transfected with the B10-hTAF$_{II}$28 expression vector but not with the TBP expression vector, whereas the converse was observed for TBP (Figure 5A, lanes 1 and 4). Both TBP and B10-hTAF$_{II}$28 were detected in extracts from cells cotransfected with the corresponding expression vectors (Figure 5A, lanes 7 and 13). The cell extracts were then immunoprecipitated with either mAb B10 or mAb 3G3. In the absence of cotransfected TBP, B10-hTAF$_{II}$28 was immunoprecipitated by mAb B10, but not by mAb 3G3 (Figure 5A, lanes 2 and 3). Similarly, in the absence of cotransfected B10-hTAF$_{II}$28, TBP was immunoprecipitated with mAb 3G3, but not with mAb B10 (Figure 5A, lanes 5 and 6). Clearly, however, when both proteins were coexpressed, TBP and B10-hTAF$_{II}$28 could be coimmunoprecipitated by either of the two mAbs (Figure 5A, lanes 8, 9, 14 and 15).

To determine whether the observed coprecipitation of B10-hTAF$_{II}$28 and TBP resulted from an intracellular interaction, or whether the two proteins simply associated with one another after cell disruption, we mixed extracts from cells transfected with B10-hTAF$_{II}$28 with extracts from cells transfected with TBP. In contrast to the efficient coimmunoprecipitation observed in the extracts from cotransfected cells (Figure 5A, lanes 8, 9, 14 and 15), almost no coimmunoprecipitation (Figure 5A, lanes 11 and 12) could be observed when the extracts of independently transfected cells were mixed together (Figure 5A, lane 10). Although this absence of coimmunoprecipitation may seem to contradict the results of the *in vitro* protein affinity chromatography experiments, it should be noted that in the *in vitro* experiments the GST fusion protein is present at high concentrations and is immobilized, whereas in the transfected cell extracts both proteins are in solution and are present in lower concentrations. Thus, the hTAF$_{II}$28–TBP interactions observed in the above coimmunoprecipitations correspond to interactions occurring intracellularly.

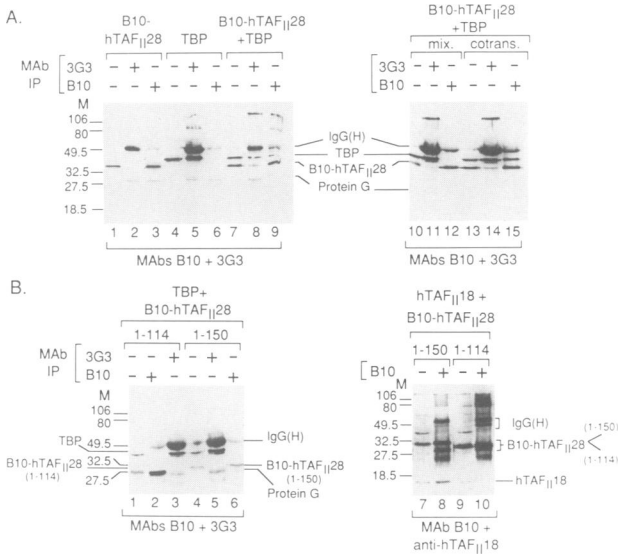

Fig. 5. (**A**) Intracellular interaction between hTAF$_{II}$28 and TBP. Aliquots of extracts from COS cells transfected with 5 μg of the expression vectors for B10-hTAF$_{II}$28 (lane 1) or TBP (lane 4), or simultaneously with both vectors (lanes 7 and 13), are shown. The cell extracts were immunoprecipitated with 1–2 μg of either the anti-tag mAb B10 or the anti-TBP mAb 3G3, as indicated above each lane. The immunoprecipitated proteins were detected on Western blots with a mixture of mAbs 3G3 and B10, indicated below the panels. The positions of TBP, B10-hTAF$_{II}$28, the protein G released from the protein G–Sepharose upon boiling of the sample, and the heavy chain of the mAbs are indicated. In lanes 10–12 extracts from cells transfected with either hTAF$_{II}$28 or TBP were mixed together, whereas in lanes 13–15 the expression vectors for each protein were cotransfected. (**B**) Distinct regions of hTAF$_{II}$28 are required for intracellular interaction with TBP and hTAF$_{II}$18. Cells were transfected with the expression vectors for the proteins indicated above each panel and the cell extracts were precipitated as described above with the mAbs indicated above each lane. The antibodies used to detect the precipitated proteins are indicated below each panel. The positions of TBP, native hTAF$_{II}$18 and the B10-hTAF$_{II}$28 deletion mutants are indicated. In lanes 7–10 native hTAF$_{II}$18 was detected using the mouse antisera raised against GST–hTAF$_{II}$18 (see also Figure 3B).

A similar strategy was also used to detect intracellular interactions between hTAF$_{II}$28 and hTAF$_{II}$18. COS cells were cotransfected with vectors expressing B10-hTAF$_{II}$18 and hTAF$_{II}$28. hTAF$_{II}$28 was detected on Western blots of transfected cell extracts using a monoclonal antibody (mAb 1C9) raised against one of the tryptic peptides derived from hTAF$_{II}$28 (see above and Materials and methods; Figure 6A, lane 1). In the absence of B10-hTAF$_{II}$18, hTAF$_{II}$28 was not immunoprecipitated by mAb B10 (Figure 6A, lane 2), whereas hTAF$_{II}$28 was efficiently precipitated by mAb B10 in the presence of cotransfected B10-hTAF$_{II}$18 (Figure 6A, lanes 3 and 4). The converse experiment could not be performed as mAb 1C9 did not immunoprecipitate hTAF$_{II}$28 (data not shown). In contrast, and in agreement with the fact that we did not detect an interaction between hTAF$_{II}$28 and hTAF$_{II}$30 (see above), hTAF$_{II}$30 and B10-hTAF$_{II}$28 did not coimmunoprecipitate from cotransfected cell extracts (Figure 6B, lanes 1–3). However, as expected, hTAF$_{II}$30 was coimmunoprecipitated with B10-hTAF$_{II}$18 (Figure 6C), but no coprecipitation of B10-hTAF$_{II}$18 and TBP could be detected (data not shown).

Taken together, these results indicate that intracellular interactions can be detected between hTAF$_{II}$28 and TBP or hTAF$_{II}$18, but not with hTAF$_{II}$30, and between hTAF$_{II}$18 and hTAF$_{II}$30.

hTAF$_{II}$20 interacts intracellularly with TBP, hTAF$_{II}$30 and hTAF$_{II}$28

A vector expressing B10-hTAF$_{II}$20 was also transfected into COS cells. Although this protein was expressed less efficiently than the other hTAF$_{II}$s, TBP could be coprecipitated with B10-hTAF$_{II}$20 (Figure 6D, lanes 1 and 2). Similarly, consistent with the *in vitro* results, hTAF$_{II}$30 could also be coimmunoprecipitated with B10-hTAF$_{II}$20 (Figure 6D, lanes 3 and 4). Conversely, coimmunoprecipitation of B10-hTAF$_{II}$20 with mAb 3G3 or 2F4 was also observed (data not shown). Interestingly, although no interaction between hTAF$_{II}$20 and hTAF$_{II}$28 could be observed *in vitro* (see above), hTAF$_{II}$28 was coimmunoprecipitated with B10-hTAF$_{II}$20 (Figure 6D, lanes 5 and 6). Thus, hTAF$_{II}$20 appears to interact intracellularly not only with TBP and hTAF$_{II}$30, but also with hTAF$_{II}$28.

Different regions of hTAF$_{II}$28 are required for interaction with TBP and hTAF$_{II}$18

A series of C- or N-terminal deletions was created in hTAF$_{II}$28 (Figure 7A) to determine the region(s) required for interactions with hTAF$_{II}$18 and TBP. The mutant proteins were expressed in *E.coli* as GST fusions, immobilized on glutathione beads and incubated with *in vitro*-translated TBP or hTAF$_{II}$18. TBP bound to wild-type GST–hTAF$_{II}$28 as well as to the two N-terminal deletion mutants (Figure 7C, lanes 1–3). In contrast, only weak binding of TBP to the C-terminal deletion mutants was observed (Figure 7C, lanes 4 and 5). Similarly, *in vitro*-translated hTAF$_{II}$18 bound efficiently to wild-type GST–hTAF$_{II}$28 and to the two N-terminal deletion mutants, but not to the C-terminal deletion mutants (Figure 7D). Thus, a domain(s) located within or overlapping with the C-terminal moiety of hTAF$_{II}$28 is required for binding *in vitro* to both hTAF$_{II}$18 and TBP.

The hTAF$_{II}$28 deletion mutants were also expressed as B10-tagged proteins in COS cells to determine the region of hTAF$_{II}$28 required for intracellular interaction with TBP. Following transfection into COS cells, the two C-terminal deletion mutants of hTAF$_{II}$28 could be detected (Figure 5B, lanes 1 and 4), and immunofluorescence indicated nuclear localization of these proteins (data not shown); however, no stable accumulation of the N-terminally deleted hTAF$_{II}$28 mutants was detected (data not shown). In agreement with the *in vitro* data, TBP was coimmunoprecipitated with wild-type hTAF$_{II}$28, but not with either of the C-terminally deleted hTAF$_{II}$28 proteins (compare Figure 5A, lanes 8, 9, 14 and 15, with B, lanes 2, 3, 5 and 6). These results indicate that an interaction surface required for intracellular association with TBP is located within, or overlapping with, the C-terminal 61 amino acids of hTAF$_{II}$28.

The B10-tagged C-terminal deletion mutants of hTAF$_{II}$28 were also coexpressed with hTAF$_{II}$18. In contrast to the results obtained *in vitro*, hTAF$_{II}$18 could be coimmunoprecipitated with B10-hTAF$_{II}$28(1–150), whereas no coimmunoprecipitation with B10-hTAF$_{II}$28(1–114) could be detected (Figure 5B, compare lanes 7 and 8 with 9 and 10). Thus, a domain located within or overlapping

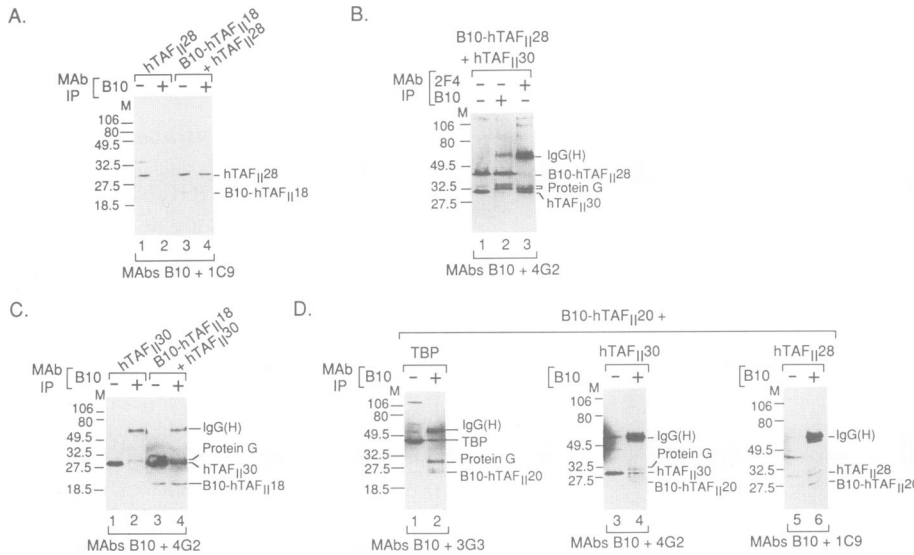

Fig. 6. (**A**) Intracellular interactions between hTAF$_{II}$28 and hTAF$_{II}$18. Cells were transfected with the expression vectors for the proteins indicated above the panel. The cell extracts were immunoprecipitated with the B10 antibody and the proteins were detected with a mixture of mAb B10 and the anti-hTAF$_{II}$28 mAb 1C9. (**B**) hTAF$_{II}$28 does not associate intracellularly with hTAF$_{II}$30. Cells were transfected with the expression vectors for the proteins indicated above the panel. Following immunoprecipitation the proteins were detected with a mixture of mAbs B10 and 4G2. (**C**) hTAF$_{II}$30 associates intracellularly with hTAF$_{II}$18. Cells were transfected with the expression vectors for the proteins indicated above the panel and immunoprecipitations were performed with mAb B10. The immunoprecipitated proteins were detected by mAbs B10 and 4G2. (**D**) Intracellular association of hTAF$_{II}$20 with TBP, hTAF$_{II}$30 and hTAF$_{II}$28. Cells were cotransfected with B10-hTAF$_{II}$20 and TBP, hTAF$_{II}$30 or hTAF$_{II}$28, as indicated above each panel. The cell extracts were precipitated with mAb B10. The immunoprecipitated proteins were detected using a mixture of mAbs B10 and 3G3 (lanes 1 and 2), B10 and 4G2 (lanes 3 and 4), and B10 and 1C9 (lanes 5 and 6).

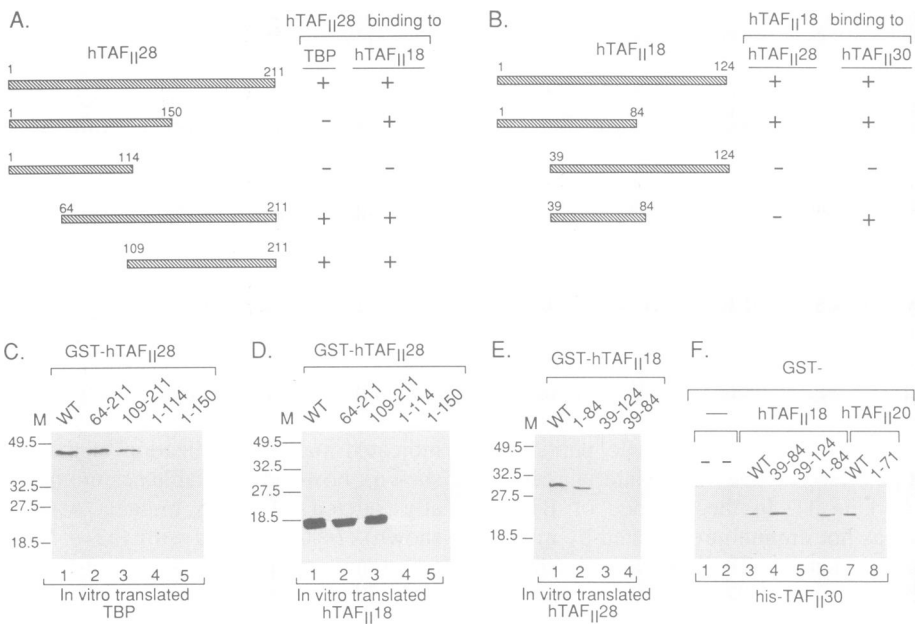

Fig. 7. (**A** and **B**) Deletion mutants in hTAF$_{II}$28 and hTAF$_{II}$18. The N- and C-terminal deletions in hTAF$_{II}$28 and hTAF$_{II}$18 are schematized. The numbers above the hatched bars indicate the amino acids at the end points of the deletions. The abilities of the wild-type and mutant proteins to interact with TBP, hTAF$_{II}$28, hTAF$_{II}$18 or hTAF$_{II}$30 in the protein affinity and/or immunoprecipitation assays are summarized to the right. +, binding; −, no binding. (**C** and **D**) *In vitro* binding of hTAF$_{II}$18 and TBP to hTAF$_{II}$28 deletion mutants. Protein affinity chromatography was performed as described in the legend to Figure 4B using ~2 μg of each of the fusion proteins and the *in vitro*-translated TBP or hTAF$_{II}$18, as indicated. In these experiments the glutathione−Sepharose beads were washed four times with buffer A containing 0.5 M KCl. WT is the full-length wild-type protein and M is the molecular mass marker. (**E**) *In vitro* binding of hTAF$_{II}$28 to hTAF$_{II}$18 deletion mutants. Protein affinity chromatography was performed using ~2 μg of each of the hTAF$_{II}$18 mutant fusion proteins and *in vitro*-translated hTAF$_{II}$28. (**F**) *In vitro* interactions between hTAF$_{II}$30, hTAF$_{II}$18 and hTAF$_{II}$20. Protein affinity chromatography was performed as described in the legend to Figure 4B except that 250 ng of purified histidine-tagged hTAF$_{II}$30 were used rather than *in vitro*-translated protein. The glutathione−Sepharose beads were washed with buffer A containing 0.5 M KCl. Lanes 1 and 2 show the results obtained with the GST protein alone; lanes 3–6 show the results with wild-type and mutant derivatives of GST−hTAF$_{II}$18; lanes 7 and 8 show the results with wild-type or a C-terminal mutant of GST−hTAF$_{II}$20. hTAF$_{II}$30 was detected using mAb 4G2.

with amino acids 114–150 of $hTAF_{II}28$ is required for intracellular interaction with $hTAF_{II}18$. Furthermore, the differential binding of $hTAF_{II}18$ and TBP to $hTAF_{II}28$(1–150) indicates that the domains of $hTAF_{II}28$ responsible for these intracellular interactions are not identical.

$hTAF_{II}28$ and $hTAF_{II}30$ interact in vitro with distinct domains of $hTAF_{II}18$

To determine the regions of $hTAF_{II}18$ required for the interactions with $hTAF_{II}28$ and $hTAF_{II}30$ *in vitro*, a series of deletion mutants was generated (Figure 7B) and fused to GST. *In vitro*-translated $hTAF_{II}28$ bound to wild-type GST–$hTAF_{II}18$ and to the C-terminal deletion mutant (1–84) (Figure 7E, lanes 1 and 2). In contrast, no binding to the N-terminal deletion mutant (39–124) or the double N- and C-terminal deletion mutant (39–84) was detected (Figure 7E, lanes 3 and 4). These results indicate that a domain within or overlapping with the N-terminal 38 amino acids of $hTAF_{II}18$ is required for interaction with $hTAF_{II}28$ *in vitro*.

E.coli-expressed his-$hTAF_{II}30$ bound to the wild-type GST–$hTAF_{II}18$, to the C-terminal deletion mutant and to the double C- and N-terminal deletion mutant (Figure 7F, lanes 3, 6 and 4, respectively). Surprisingly, however, no binding to the N-terminal deletion mutant (39–124) was detected (Figure 7F, lane 5). Nevertheless, amino acids 39–84 of $hTAF_{II}18$ sufficed to interact with $hTAF_{II}30$, but not with $hTAF_{II}28$ (compare Figure 7F, lane 4, with E, lane 4). Thus, distinct regions of $hTAF_{II}18$ are required for interaction with $hTAF_{II}30$ and $hTAF_{II}28$.

Discussion

hTFIIDα and hTFIIDβ have distinct $hTAF_{II}$ compositions

We report here the cloning of cDNAs encoding three subunits of hTFIID. $hTAF_{II}28$ is the homologue of the previously characterized $dTAF_{II}30\beta$, while $hTAF_{II}20$ is the homologue of p22. In *Drosophila*, p22 is an alternatively spliced form of $dTAF_{II}30\alpha$ (Kokubo *et al.*, 1994). However, none of the $hTAF_{II}20$ cDNAs from HeLa cells isolated in this study encoded a protein analogous to $dTAF_{II}30\alpha$. The detection of a human homologue of full-length $dTAF_{II}30\alpha$ and the determination of its abundance and distribution in different human cell lines will be facilitated by the development of antibodies against $hTAF_{II}20$.

The amino acid sequence of $hTAF_{II}18$ shows homology to the N-terminal region of the yeast TAF_{II} SPT3 (Eisenmann *et al.*, 1992, and references therein). A more extensive homology between $hTAF_{II}18$ and the yeast protein FUN 81 (Dubois *et al.*, 1987) was observed, suggesting that this protein may also be a yeast TAF_{II}. Recently, other yeast TAF_{II}s with homology to d(h)$TAF_{II}250$ and $dTAF_{II}80$ have been reported (Reese *et al.*, 1994). However, no homologue of $hTAF_{II}18$ has been described in *Drosophila* as yet. This result, together with the fact that no *Drosophila* homologue of $hTAF_{II}30$ has been identified, supports the idea that hTFIID may comprise more TAF_{II}s than dTFIID. Nevertheless, one cannot exclude the existence of *Drosophila* counterparts for these $hTAF_{II}$s as such counterparts may correspond to cell-specific $dTAF_{II}$s expressed in *Drosophila* adult tissues.

We showed previously that hTFIID complexes could be separated into two species, hTFIIDα and hTFIIDβ, either lacking or containing $hTAF_{II}30$ (Jacq *et al.*, 1994). These two species appeared to comprise both core and specific $hTAF_{II}$s. From these results we proposed that $hTAF_{II}28$ would be a core $hTAF_{II}$, but that $hTAF_{II}18$ and $hTAF_{II}20$ would be specifically associated with TFIIDβ. However, we could not formally demonstrate that the 28 kDa subunits detected in both TFIIDα and TFIIDβ were in fact the same protein rather than two distinct proteins with analogous electrophoretic mobilities. Using antibodies against recombinant $hTAF_{II}28$, we show here that $hTAF_{II}28$ is indeed a core TAF_{II} present in both TFIIDα and TFIIDβ. Thus, we conclude from this and our previous study (Jacq *et al.*, 1994) that $hTAF_{II}250$, $hTAF_{II}100$ and $hTAF_{II}28$ are core $hTAF_{II}$s common to both TFIIDα and TFIIDβ.

In contrast to $hTAF_{II}28$, we show that $hTAF_{II}18$ is preferentially, if not exclusively, associated with TFIIDβ, confirming our previous proposal that $hTAF_{II}18$ is a TFIIDβ-specific $hTAF_{II}$ (Jacq *et al.*, 1994). These results show clearly that TFIIDα and TFIIDβ have distinct $hTAF_{II}$ compositions, as they differ not only by the presence or absence of $hTAF_{II}30$, but also by that of $hTAF_{II}18$. Antibodies directed against recombinant $hTAF_{II}20$ will be required to demonstrate that the isolated $hTAF_{II}20$ cDNA, characterized here, encodes the 20 kDa TFIID subunit which we have proposed to be a TFIIDβ-specific TAF_{II} (Jacq *et al.*, 1994).

$hTAF_{II}18$ interacts directly with TBP but interacts more strongly with $hTAF_{II}30$ and $hTAF_{II}28$, both of which also interact directly with TBP (summarized in Figure 8A and B). As $hTAF_{II}18$ interacts with $hTAF_{II}28$ and $hTAF_{II}30$ it is conceivable that it would be recruited more stably to TFIIDβ containing both $hTAF_{II}28$ and $hTAF_{II}30$, in agreement with the observation that $hTAF_{II}18$ is a TFIIDβ-specific TAF_{II}. Similarly, $hTAF_{II}30$ may be more stably associated with TFIIDβ due to interactions with both TBP and $hTAF_{II}18$. Alternatively, the TFIIDβ-specific $hTAF_{II}$s, $hTAF_{II}30$, $hTAF_{II}18$ and $hTAF_{II}20$, may interact to preform a ternary complex, which is then recruited by interactions with the core $hTAF_{II}$s and TBP to form TFIIDβ. Reconstitution experiments will be required to test these possibilities.

TAF–TAF and TAF–TBP interactions in hTFIID

In this study we have identified a series of *in vitro* and intracellular interactions amongst the novel $hTAF_{II}$s, and between the novel $hTAF_{II}$s and $hTAF_{II}30$ or TBP. We have shown that $hTAF_{II}28$ and $hTAF_{II}20$ interact with TBP both *in vitro* and intracellularly following transient cotransfection. It is important to note that the intracellular interactions detected in the cotransfection experiments do not result from the incorporation of the transfected $hTAF_{II}$s or TBP into the endogenous COS cell TFIID. This is clearly indicated by the absence of coprecipitation of transfected $hTAF_{II}28$ and $hTAF_{II}30$, despite the fact that these proteins are associated in TFIIDβ. Similarly, no coprecipitation of the endogenous COS cell TBP and transfected $hTAF_{II}$s was observed. Moreover, when extracts from cells cotransfected with TBP and $hTAF_{II}28$ were precipitated with an anti-TBP mAb, no $hTAF_{II}$s other

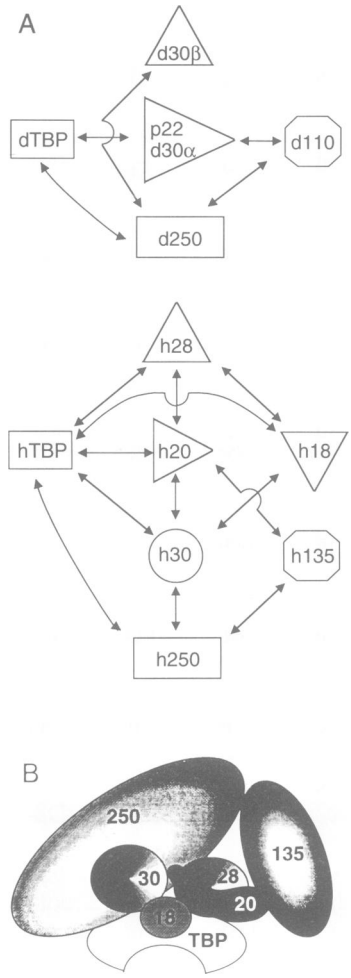

Fig. 8. (**A**) Comparison of TAF–TAF and TAF–TBP interactions in hTFIID and dTFIID. The arrows in the upper panel show TAF–TAF and TAF–TBP contacts in dTFIID (see Chen *et al.*, 1994, and references therein). The arrows in the lower panel show TAF–TAF and TAF–TBP contacts in hTFIID. Only $dTAF_{II}$s homologous to the $hTAF_{II}$s studied here and in Jacq *et al.* (1994) are shown. The homologous human and *Drosophila* proteins are located in similar positions relative to TBP and boxed in the same fashion. (**B**) Summary of the protein–protein contacts within hTFIIDβ. The TAF–TAF and TAF–TBP interactions deduced from this and previous studies are summarized. $hTAF_{II}250$, $hTAF_{II}30$, $hTAF_{II}28$, $hTAF_{II}20$ and $hTAF_{II}18$ interact with TBP. $hTAF_{II}250$ interacts with $hTAF_{II}135$ and $hTAF_{II}30$. In addition, $hTAF_{II}30$ also contacts $hTAF_{II}20$ and $hTAF_{II}18$. $hTAF_{II}28$ interacts with $hTAF_{II}18$ and $hTAF_{II}20$ and, in addition, $hTAF_{II}20$ contacts $hTAF_{II}30$ and $hTAF_{II}135$. Note that the $hTAF_{II}$s are shown to contact TBP simultaneously, but this has not been demonstrated experimentally. Alternatively, TFIID complexes may be formed by several different pathways.

than $hTAF_{II}28$ could be detected by either immunoblotting or silver nitrate staining (our unpublished data).

Our results and those from other laboratories show clearly that, contrary to initial reports (Hisatake *et al.*, 1993; Kokubo *et al.*, 1993a; Zhou *et al.*, 1993), $TAF_{II}250$ is not the only TAF_{II} to interact directly with TBP. In dTFIID, $dTAF_{II}250$, $dTAF_{II}30\alpha$ and $dTAF_{II}150$ have all been shown to interact directly with dTBP. For $dTAF_{II}40$ (p42), $dTAF_{II}60$ (p62) and $dTAF_{II}80$ (p85) contradictory results concerning their ability to bind to dTBP have been obtained (Goodrich *et al.*, 1993; Weinzierl *et al.*, 1993a; Chen *et al.*, 1994; Kokubo *et al.*, 1994). In hTFIID, $hTAF_{II}250$, $hTAF_{II}30$, $hTAF_{II}28$, $hTAF_{II}20$ and $hTAF_{II}18$ have been shown to interact with hTBP (Figure 8A and B). In addition, Zhou *et al.* (1993) reported that an as yet uncharacterized $hTAF_{II}125$ also interacted with TBP in far Western blotting experiments, although it is not known whether $hTAF_{II}125$ is a homologue of $dTAF_{II}150$ or simply a degradation product of $hTAF_{II}250$. It will be interesting to determine with which regions of TBP each of these TAF_{II}s interacts, and whether they can all interact simultaneously with TBP or whether some of these interactions are mutually exclusive. Recently it has been shown that the binding of $dTAF_{II}250$ and $dTAF_{II}150$ to TBP prevented the subsequent interaction with the $hTAF_{I}$s and vice versa (Comai *et al.*, 1994). It is possible that there may also be a competition between the $hTAF_{II}$s for binding to TBP, suggesting that hTFIID complexes may be assembled by more than one pathway.

In addition to TBP, $hTAF_{II}28$ also interacts with $hTAF_{II}18$ (Figure 8A and B). Deletion analysis indicated that the C-terminal region of $hTAF_{II}28$ (amino acids 109–211) bound TBP, and that deletion of the C-terminal 61 amino acids abolished binding to TBP. These results indicate that a region within or overlapping with the C-terminal 61 amino acids of $hTAF_{II}28$ contains an interaction surface required for binding to TBP.

The C-terminal amino acids 109–211 of $hTAF_{II}28$ also bound *in vitro* to $hTAF_{II}18$, and no binding of $hTAF_{II}18$ to the two C-terminal deletion mutants was observed *in vitro*. However, in transfected cells $hTAF_{II}18$ interacted with the C-terminal deletion mutant (1–150) but not with mutant (1–114), whereas neither of these mutants bound TBP. The differential binding of $hTAF_{II}18$ and TBP to mutant (1–150) in the same intracellular assay indicates that these two proteins bind, at least in part, to distinct regions of $hTAF_{II}28$. Note that there is a difference in the ability of $hTAF_{II}18$ to bind to the C-terminal deletion 1–150 *in vitro* and intracellularly. We have observed another discrepancy between the intracellular and *in vitro* results as no *in vitro* binding between $hTAF_{II}20$ and $hTAF_{II}28$ was observed, but these two $hTAF_{II}$s were coprecipitated from cotransfected cells. Some of these observations may be explained by the bacterially produced GST fusion proteins adopting conformations which artefactually mask potential interaction surfaces. Alternatively, intracellular post-translational modifications, such as phosphorylation, may be required to allow interaction between $hTAF_{II}28$ and $hTAF_{II}20$. In this respect we note that many $hTAF_{II}$s have been shown to be phosphorylated (Boyer and Berk, 1993). Furthermore, although the intracellular TAF–TAF interactions described here do not result from the incorporation of the transfected $hTAF_{II}$s into TFIID complexes, we cannot exclude the possibility that some of these interactions may be mediated by unknown bridging proteins. In view of such observations, negative results in *in vitro* assays should not be taken as definitive proof of a lack of interaction between two proteins.

$hTAF_{II}18$ interacts with $hTAF_{II}30$ and $hTAF_{II}28$ (Figure 8A and B). Deletion analysis indicates that the N-terminal 38 amino acids of $hTAF_{II}18$ are required for interaction with $hTAF_{II}28$. Furthermore, although no binding of $hTAF_{II}30$ to the N-terminal deletion mutant (39–124) was observed (possibly due to artefactual folding of the bacterially expressed protein; discussed above), amino acids 39–84 sufficed to interact with $hTAF_{II}30$. Thus, in

the same *in vitro* assay, mutant (39–84) had a differential ability to bind $hTAF_{II}30$ and $hTAF_{II}28$, indicating that distinct domains within $hTAF_{II}18$ are required for interactions with these two $hTAF_{II}$s. Analogous experiments were not performed in transient transfection assays as the B10-tagged $hTAF_{II}18$ deletion mutants did not accumulate in transfected cells (our unpublished data).

Comparison of TAF–TAF and TAF–TBP interactions in hTFIID and dTFIID

Comparison of the results of our present and previous hTFIID studies (Jacq *et al.*, 1994) with those concerning dTFIID reveals a number of similarities and differences in the organization of TFIID complexes in *Drosophila* embryos and human HeLa cells (summarized in Figure 8A). As discussed above, the major difference is the existence in HeLa cell TFIID of two $hTAF_{II}$s with no known *Drosophila* homologues. Nevertheless, major differences exist even for homologous TAF_{II}s. The most striking of these concerns $hTAF_{II}28$ which interacts with hTBP but not $hTAF_{II}250$, whereas its *Drosophila* homologue interacts with $dTAF_{II}250$ but not dTBP (Yokomori *et al.*, 1993b; Chen *et al.*, 1994; see Figure 8A).

On the other hand, and in agreement with the results obtained with p22 and $dTAF_{II}30\alpha$ (Yokomori *et al.*, 1993b; Kokubo *et al.*, 1994), $hTAF_{II}20$ interacts directly with TBP and with $hTAF_{II}135$, the human homologue of $dTAF_{II}110$ (Hoey *et al.*, 1993; Yokomori *et al.*, 1993b; our unpublished data; summarized in Figure 8A and B). However, in addition to binding to TBP and $hTAF_{II}135$, we also detected additional interactions between $hTAF_{II}20$ and $hTAF_{II}28$ or $hTAF_{II}30$. The *in vitro* experiments further suggest that $hTAF_{II}30$ and TBP (data not shown) interact with $hTAF_{II}20$ via the C-terminal moiety of $hTAF_{II}20$. This region is highly conserved between the *Drosophila* and human proteins, and sequences within this region of $dTAF_{II}30\alpha$ have been shown to be required for binding to $dTAF_{II}110$ and multimerization of $dTAF_{II}30\alpha$ (Yokomori *et al.*, 1993b). A detailed analysis of $hTAF_{II}20$ will be required to precisely determine the domains required for each of these interactions. In any event it is clear that hTFIID differs from dTFIID, as it is known at present, in a number of respects; hTFIID comprises more TAF_{II}s than dTFIID and these $hTAF_{II}$s assemble into two hTFIID species (α and β), and differing TAF–TAF and TAF–TBP interactions can be observed in hTFIID and dTFIID.

Although this study gives some new insights into the organization of hTFIID, the function of the novel $hTAF_{II}$s described here is as yet unknown. It has been suggested previously (Yokomori *et al.*, 1993b) that $dTAF_{II}30\alpha$ and β could act to stabilize contacts between the other TFIID subunits. This may also be the function of $hTAF_{II}20$ as this $hTAF_{II}$ contacts many other TFIID subunits. These observations, however, do not rule out the possibility that these small $hTAF_{II}$s may also make contacts with transcriptional activators, as observed with $hTAF_{II}30$ (Jacq *et al.*, 1994), and play a direct role in the transactivation process. Experiments to test these possibilities are currently in progress.

Materials and methods

Purification of TFIID complexes and cloning of $hTAF_{II}$s

Nuclear extracts were prepared and purified on heparin–ultrogel as described (Brou *et al.*, 1993a; Chaudhary *et al.*, 1994). The TFIID was immunopurified using the mAbs 2C1 or 3G3, and the TFIID eluted from the protein G–Sepharose using an excess of synthetic peptide comprising the corresponding epitope. The eluted TFIID was dialysed against buffer containing 5 mM NaCl, 0.5 mM Tris–HCl (pH 7.9), 5 μM DTT and 0.01% SDS for 6–8 h. The TFIID was then lyophilized and resolved by SDS–PAGE. The proteins were electroblotted overnight in 50 mM Tris and 50 mM boric acid onto a PVDF membrane (Millipore, Immobilon P, 0.45 μM) and stained briefly with Coomassie blue. The $hTAF_{II}$s were excised and digested *in situ* on the membrane with trypsin. The eluted peptides were then separated by reverse-phase HPLC and microsequenced.

For $hTAF_{II}28$, two peptides were obtained: MQILVSSFSEEQLNR and LIQSITGTSVSQNVVIAM. Based on these sequences two degenerate oligonucleotides were synthetized: 5′-ATGCAA/GATC/TC/TTIGTG/C/TT/AC/GIT/AC/GITTC/TT/AC/GIGAA/GGAA/GCAA/GC/TTIAAC/TC/AG-3′ and 5′-C/TTG/C/TATC/TCAA/GA/TC/GIATC/TACA/C/TGGA/G/C/TACA/C/TA/TC/GIGTC/GA/TC/GICAA/GAAC/TGTC/GGTC/GATC/TGCA/C/TATG-3′. They were used to screen a random-primed HeLa cell cDNA library in λ ZAPII (Stratagene). 6×10^5 clones were screened by hybridization with the ^{32}P 5′ end-labelled oligonucleotides in 6× SSC at 42°C overnight. The filters were washed in 6× SSC at 45 or 50°C and subjected to autoradiography. Three clones which hybridized with both oligonucleotides were purified and *in vivo* excision was performed. The cDNA inserts were completely sequenced with internal primers using an Applied Biosystems automated DNA sequencer. The resulting data were analysed and database searching was performed using the Genetics Computer Group (GCG) software (University of Wisconsin, WI) sequence analysis programmes.

For $hTAF_{II}20$, four peptides were obtained: DVQLHLER, QWNMWIPGFGSEEIR, LSPENNQVLTK and MALIR. Oligonucleotides corresponding to the first two sequences were synthetized and used to screen the HeLa library (5′-GAC/TGTC/T/GCAA/GC/TTICAC/TC/TTIGAA/GC/AG-3′ and 5′-CAA/GTGGAAC/TATGTGGGATC/TCCA/C/TGGITTC/TGGIA/TGCIGAA/GGAA/GATC/TC/AG-3′). The resulting clones were analysed as described above.

For $hTAF_{II}18$, two peptides were obtained: VQVEDIVFLIRK and ARKAFDEANYGS. The corresponding oligonucleotides were synthetized: 5′-GTC/G/TCAA/GGTC/G/TGAA/GGAC/TATC/TGTC/G/TTT-3′ and 5′-AAA/GGCA/C/TTTC/TGAC/TGAA/GGCA/C/TAAC/TTAC/TGG-3′.

Construction of expression vectors

The coding sequences of $hTAF_{II}28$ and $hTAF_{II}18$ and the corresponding deletion mutants were amplified by the PCR using appropriate primers with in-frame *Bam*HI and *Eco*RI sites. They were cloned into the corresponding sites in the pGEX2T vector. GST–$hTAF_{II}20$ WT and 1–71 were constructed by PCR amplifying the appropriate regions of the $hTAF_{II}20$ coding sequence with oligonucleotide primers containing in-frame *Eco*RI sites and cloning into the *Eco*RI site of pGEX2T. GST–$hTAF_{II}135$ was constructed by inserting a *Bgl*II–*Eco*RI fragment encoding the C-terminal 602 amino acids into pGEX3X. GST–TBP has been described previously (Jacq *et al.*, 1994). pXJ42–$hTAF_{II}28$, pXJ41–$hTAF_{II}20$ and pXJ41–$hTAF_{II}18$ were constructed by PCR amplifying the corresponding coding sequences with *Eco*RI and *Bam*HI sites (or *Xho*I and *Eco*RI for $hTAF_{II}20$) and cloning into the pXJ expression vectors described previously (Xiao *et al.*, 1991). The PCR primer oligonucleotides were designed to introduce a consensus Kozak sequence. pXJ41–$hTAF_{II}30$ and pXJ40–TBP were as described previously (Jacq *et al.*, 1994). Histidine-tagged $hTAF_{II}28$ and $hTAF_{II}18$ were constructed by PCR using oligonucleotide primers containing *Nde*I and *Bam*HI restriction sites. The resulting fragments were cloned between the appropriate sites in pET15.

The B10 epitope-tagged $hTAF_{II}28$, $hTAF_{II}20$ and $hTAF_{II}18$ were constructed by PCR amplifying the corresponding coding sequences with in-frame *Nhe*I sites and cloning into a modified pAT6 expression vector (Tribouley *et al.*, 1994). The DNA sequences of all plasmids were verified by automated DNA sequencing.

Immunization, mAb production, immunoprecipitation and immunoblotting

Immunizations and mAb production were performed as described previously (Brou *et al.*, 1993a; Lescure *et al.*, 1994). Mice were injected intraperitoneally three times at 2 week intervals with 100 μg of the $hTAF_{II}28$ peptide MQILVSSFSEEQLNR coupled to ovalbumin. Spleen cells were fused with Sp2/O AG 14 myeloma cells; culture supernatants at day 10 were tested on COS cells transfected with pXJ42–$hTAF_{II}28$ by immunostaining or ELISA. These injections generated mAb 1C9.

Mice were also injected three times at 2 week intervals with 200 μg purified GST–hTAF$_{II}$28 or GST–hTAF$_{II}$18 and the immunoblots in Figure 3 were performed with the resulting mouse serum. After fusions, two mAbs were obtained: 15TA against hTAF$_{II}$28 and 16TA against hTAF$_{II}$18. These mAbs were used for the immunoblots shown in Figure 4F.

The anti-TBP antibodies 3G3 and 2C1 and the anti-hTAF$_{II}$30 antibodies 4G2 and 2F4 were purified by caprylic acid and ammonium sulfate precipitation as described previously (Brou *et al.*, 1993a). mAb B10 was as described previously (Ali *et al.*, 1993).

The preparative immunopurification of TFIID complexes was essentially as described previously (Jacq *et al.*, 1994). 250 ml of the H 0.6 M KCl fraction (~500 mg of protein) were immunoprecipitated with ~300 μg of mAbs 3G3 or 2C1 using 1 ml of protein G–Sepharose overnight at 4°C. The resin was then washed extensively five times with 50 ml of buffer A (50 mM Tris–HCl, pH 7.9, 10% glycerol, 0.5 mM EDTA, 1 mM DTT and 0.2% NP-40) containing 1.0 M KCl and the TFIID eluted by the addition of an excess of the corresponding epitope peptide.

Transfected cell extracts were precipitated with 1–2 μg of mAbs B10, 3G3 or 2F4, and 30–40 μl of protein G–Sepharose for 2 h at 4°C. The resin was then washed four times for 10 min at 20°C with 1 ml buffer A containing 1.0 M KCl. The resin was then boiled in SDS loading buffer and the proteins separated by SDS–PAGE.

Western blot analyses were performed by standard methods using an ECL kit (Amersham).

In vitro transcription and translation

In vitro transcription and translation were performed as described previously (Hwang *et al.*, 1993). Plasmids were linearized at appropriate restriction sites and 2 μg were transcribed with T7 RNA polymerase. 100–500 ng of the resulting RNA were translated in the presence of [^{35}S]methionine in 35 μl of a rabbit reticulocyte lysate in a final volume of 50 μl. A 1 μl aliquot of the translation products was separated by SDS–PAGE. The gels were fixed with 100% acetic acid and then treated with 10% 2-5 diphenyloxazole (PPO) in acetic acid. The gels were then washed with water, dried and subjected to autoradiography.

Protein affinity chromatography

E.coli cells harbouring the GST–TAF (TBP) fusion vectors were induced for 2–3 h at 37°C with 1 mM IPTG. The cells were lysed by sonication in buffer A containing 500 mM KCl; the insoluble material was removed by centrifugation at 25 000 r.p.m. for 20 min. 100 μl–1 ml of the extracts were then incubated for 2 h at 4°C with 50 μl of glutathione–Sepharose beads. The beads were collected by centrifugation and washed four times with 1 ml of buffer A containing 1.0 M KCl. The bound protein was detected by staining with Coomassie blue following SDS–PAGE. The amounts of cell extracts required to immobilize 1–2 μg of each GST fusion protein were then determined. Alternatively, the fusion proteins used for immunization of mice were eluted from the beads using buffer A containing 10 mM reduced glutathione. For protein affinity chromatography, the immobilized GST fusion proteins were washed as described above and incubated with either the *in vitro*-translated proteins or purified his-TAF$_{II}$s in a 100 μl volume for 2 h at 4°C with nutation. The beads were then washed four times for 10 min at 20°C with 1 ml of buffer A containing 0.1 M KCl. Half of the beads were then removed and added to 30 μl SDS loading buffer. The remaining beads were then washed three times with 1 ml buffer A containing 0.5 M KCl prior to SDS–PAGE. The gels were fixed and dried as described above and subjected to autoradiography. His-tagged hTAF$_{II}$s were expressed and purified as described previously (Jacq *et al.*, 1994). Following binding experiments, the his-TAF$_{II}$s were detected by immunoblotting using the appropriate mAbs.

Transient transfections and cell extracts

COS cells were transfected with 2–10 μg of the pAT6 or pXJ40 series expression vectors by the calcium phosphate coprecipitation method. 48 h after transfection the cells were washed with PBS and harvested. Cells from a 1×90 mm plate were lysed by the addition of 100 μl of buffer A containing 0.5 M KCl, followed by three rounds of freezing and thawing. 50 μl of the cell extracts were then used in the immunoprecipitations.

Acknowledgements

We thank R.Tjian, M.Vigneron, J.Acker and J.-M.Garnier for the gift of recombinants and the HeLa cell cDNA library, J.Acker for the gift of labelled hTAF$_{II}$250, R.Fraser and E.Remboutsika for critical reading of the manuscript, M.-E.Valentin and L.Carré for excellent technical assistance, Y.Lutz and the Monoclonal Antibody Facility for mAbs and immunofluorescence, the staff of the Cell Culture Facility for HeLa and COS cells, the staff of the oligonucleotide facility for oligonucleotides, P.Eberling for peptide synthesis, S.Vicaire for automated DNA sequencing, and G.Eisenmann for baculovirus-expressed hTAF$_{II}$250. We also thank J.-M.Lafontaine, C.Werlé and R.Bucher for artwork. The sequences described in this paper have been assigned the following accession numbers: hTAF$_{II}$28, X83928; hTAF$_{II}$20, X84002; and hTAF$_{II}$18, X84003. M.M. was supported by a grant from the Deutsche Forschungsgemeinschaft (DFG). This work was supported by grants from the CNRS, the INSERM, the Centre Hospitalier Universitaire Régional, the Ministère de la Recherche et de la Technologie, the Association pour la Recherche contre le Cancer and the Collège de France.

References

Ali,S., Lutz,Y., Bellocq,J.-P., Chenard-Neu,M.-P., Rouyer,N. and Metzger,D. (1993) *Hybridoma*, **12**, 391–405.

Arlas,J., Alberts,A.S., Brindle,P., Claret,F.X., Smeal,T., Karin,M., Feramisco,J. and Montminy,M. (1994) *Nature*, **370**, 229–229.

Boyer,T.G. and Berk,A.J. (1993) *Genes Dev.*, **7**, 1810–1823.

Brou,C., Chaudhary,S., Davidson,I., Lutz,Y., Wu,J., Egly,J.-M., Tora,L. and Chambon,P. (1993a) *EMBO J.*, **12**, 489–499.

Brou,C., Wu,J., Ali,S., Scheer,E., Lang,C., Davidson,I., Chambon,P. and Tora,L. (1993b) *Nucleic Acids Res.*, **21**, 5–12.

Buratowski,S. (1994) *Cell*, **77**, 1–3.

Chaudhary,S., Brou,C., Valentin,M.E., Burton,N., Tora,L., Chambon,P. and Davidson,I. (1994) *Mol. Cell. Biol.*, **14**, 5290–5299.

Chen,J.L., Attardi,L.D., Verrijzer,C.P., Yokomori,K. and Tjian,R. (1994) *Cell*, **79**, 93–105.

Chiang,C.M., Ge,H., Wang,Z., Hoffmann,A. and Roeder,R.G. (1993) *EMBO J.*, **12**, 2749–2762.

Comai,L., Zomerdijk,J.B.C.M., Beckman,H., Zhou,S., Admon,A. and Tjian,R. (1994) *Science*, **266**, 1966–1969.

Conaway,R.C. and Conaway,J.W. (1993) *Annu. Rev. Biochem.*, **62**, 161–190.

DeJong,J. and Roeder,R.G. (1993) *Genes Dev.*, **7**, 2220–2234.

Dubois,E., Bercy,J., Descamps,F. and Messenguy,F. (1987) *Gene*, **55**, 265–275.

Dynlacht,B.D., Hoey,T. and Tjian,R. (1991) *Cell*, **66**, 563–576.

Dynlacht,B.D., Weinzierl,R.O.J., Admon,A. and Tjian,R. (1993) *Nature*, **363**, 176–179.

Eisenmann,D.M., Arndt,K.M., Ricupero,S.L., Rooney,J.W. and Winston,F. (1992) *Genes Dev.*, **6**, 1319–1331.

Ge,H. and Roeder,R.G. (1994) *Cell*, **78**, 513–523.

Gill,G. and Tjian,R. (1992) *Curr. Opin. Genet. Dev.*, **2**, 236–242.

Gill,G., Pascal,E., Tseng,Z.H. and Tjian,R. (1994) *Proc. Natl Acad. Sci. USA*, **91**, 192–196.

Goodrich,J.A., Hoey,T., Thut,C.J., Admon,A. and Tjian,R. (1993) *Cell*, **75**, 519–530.

Hernandez,N. (1993) *Genes Dev.*, **7**, 1291–1308.

Hisatake,K., Hasegawa,S., Takada,R., Nakatani,Y., Horikoshi,M. and Tjian,R. (1993) *Nature*, **362**, 179–181.

Hoey,T., Weinzierl,R.O., Gill,G., Chen,J.L., Dynlacht,B.D. and Tjian,R. (1993) *Cell*, **72**, 247–260.

Hwang,J.J., Chambon,P. and Davidson,I. (1993) *EMBO J.*, **12**, 2337–2348.

Jacq,X., Brou,C., Lutz,Y., Davidson,I., Chambon,P. and Tora,L. (1994) *Cell*, **79**, 107–117.

Jupp,R., Flores,O., Nelson,J.A. and Ghazal,P. (1993) *J. Biol. Chem.*, **268**, 16105–16108.

Kato,K., Makino,Y., Kishimoto,T., Yamauchi,J., Kato,S., Muramatsu,M. and Tamura,T.-A. (1994) *Nucleic Acids Res.*, **22**, 1179–1185.

Kokubo,T., Takada,R., Yamashita,S., Gong,D.-W., Roeder,R.G., Horikoshi,M. and Nakatani,Y. (1993a) *J. Biol. Chem.*, **23**, 17554–17558.

Kokubo,T., Gong,D.-W., Roeder,R.G., Horikoshi,M. and Nakatani,Y. (1993b) *Proc. Natl Acad. Sci. USA*, **90**, 5896–5900.

Kokubo,T., Gong,D.W., Wooton,J.C., Horikoshi,M., Roeder,R.G. and Nakatani,Y. (1994) *Nature*, **367**, 484–487.

Kretzschmar,M., Kaiser,K., Lottspeich,F. and Meisterernst,M. (1994a) *Cell*, **78**, 525–534.

Kretzschmar,M., Stelzer,G., Roeder,R.G. and Meisterernst,M. (1994b) *Mol. Cell. Biol.*, **14**, 3927–3937.

Kwok,R.P.S., Lundblad,J.R., Chrivia,J.C., Richards,J.P., Bächinger,H.P., Brennan,R.G., Roberts,S.G.E., Green,M.G. and Goodman,R.H. (1994) *Nature*, **370**, 223–226.
Lescure,A., Lutz,Y., Eberhardt,D., Jacq,X., Krol,A., Grummt,I., Davidson,I., Chambon,P. and Tora,L. (1994) *EMBO J.*, **13**, 1166–1175.
Lieberman,P.M. and Berk,A.J. (1994) *Genes Dev.*, **8**, 995–1006.
Ma,D. *et al.* (1993) *Genes Dev.*, **7**, 2246–2257.
Marcus,G.A., Silverman,N., Berger,S.L., Horiuchi,J. and Guarente,L. (1994) *EMBO J.*, **13**, 4807–4815.
Ozer,J., Moore,P.A., Bolden,A.H., Lee,A., Rosen,C.A. and Lieberman,P.M. (1994) *Genes Dev.*, **8**, 2324–2335.
Pearson,W.R. and Lipman,D.J. (1988) *Proc. Natl Acad. Sci. USA*, **85**, 2444–2448.
Pierrat,B., Heery,D.M., Chambon,P. and Losson,R. (1994) *Gene*, **143**, 193–200.
Pugh,B.F. and Tjian,R. (1991) *Genes Dev.*, **5**, 1935–1945.
Pugh,B.F. and Tjian,R. (1992) *J. Biol. Chem.*, **267**, 679–682.
Reese,J.C., Apone,L., Walker,S.S., Griffin,L.A. and Green,M.R. (1994) *Nature*, **371** 523–527.
Roeder,R.G. (1991) *Trends Biochem. Sci.*, **16**, 402–408.
Ruppert,S., Wang,E.H. and Tjian,R. (1993) *Nature*, **362**, 175–179.
Sekiguchi,T., Nohiro,Y., Nakamura,Y., Hisamoto,N. and Nishimoto,T. (1991) *Mol. Cell. Biol.*, **11**, 3317–3325.
Sun,X., Ma,D., Sheldon,M., Yeung,K. and Reinberg,D. (1994) *Genes Dev.*, **8**, 2336–2348.
Tanese,N., Pugh,B.F. and Tjian,R. (1991) *Genes Dev.*, **5**, 2212–2224.
Timmers,H.M.T., Meyers,R.E. and Sharp,P. (1992) *Proc. Natl Acad. Sci. USA*, **89**, 8140–8144.
Tjian,R. and Maniatis,T. (1994) *Cell*, **79** 5–8.
Tribouley,C., Lutz,P., Staub,A. and Kedinger,C. (1994) *J. Virol.*, **68**, 4450–4457.
Verrijzer,C.P., Yokomori,K., Chen,J.-L. and Tjian,R. (1994) *Science*, **264**, 933–941.
Weinzierl,R.O.J., Ruppert,S., Dynlacht,B.D., Tanese,N. and Tjian,R. (1993a) *EMBO J.*, **12**, 5303–5309.
Weinzierl,R.O.J., Dynlacht,B.D. and Tjian,R. (1993b) *Nature*, **362**, 511–517.
Xiao,J.H., Davidson,I., Matthes,H., Garnier,J.-M. and Chambon,P. (1991) *Cell*, **65**, 551–568.
Yokomori,K., Admon,A., Goodrich,J.A., Chen,J.-L. and Tjian,R. (1993a) *Genes Dev.*, **7**, 2235–2245.
Yokomori,K., Chen,J.-L., Admon,A., Zhou,S. and Tjian,R. (1993b) *Genes Dev.*, **7**, 2587–2597.
Yokomori,K., Zeidler,M.P., Chen,J.L., Verrijzer,C.P., Mlodzik,M. and Tjian,R. (1994) *Genes Dev.*, **8**, 2313–2323.
Zhou,Q., Lieberman,P.M., Boyer,T.G. and Berk,A.J. (1992) *Genes Dev.*, **6**, 1964–1974.
Zhou,Q., Boyer,T.G. and Berk,A.J. (1993) *Genes Dev.*, **7**, 180–187.

Received on November 18, 1994; revised on January 23, 1995